Article:
Sawyer, D., Tinkler, L., Roberts, N. et al. (2020) Improving robotic accuracy through iterative teaching. SAE Technical Papers, 2020 (March). 2020-01-0014. ISSN: 0148-7191

https://doi.org/10.4271/2020-01-0014

Improving Robotic Accuracy through Iterative Teaching

Author, co-author (Do NOT enter this information. It will be pulled from participant tab in MyTechZone)

Affiliation (Do NOT enter this information. It will be pulled from participant tab in MyTechZone)

Abstract

Industrial robots have been around since the 1960s and their introduction into the manufacturing industry has helped in automating otherwise repetitive and unsafe tasks, while also increasing the performance and productivity for the companies that adopted the technology. As the majority of industrial robotic arms are deployed in repetitive tasks, the pose accuracy is much less of a key driver for the majority of consumers (e.g. the automotive industry) than speed, payload, energy efficiency and unit cost. Consequently, manufacturers of industrial robots often quote repeatability as an indication of performance whilst the pose accuracy remains comparatively poor. Due to their lack in accuracy, robotic arms have seen slower adoption in the aerospace industry where high accuracy is of utmost importance. However if their accuracy could be improved, robots offer significant advantages, being comparatively inexpensive and more flexible than bespoke automation. Extensive research has been conducted in the area of improving robotic accuracy through re-calibration of the kinematic model. This approach is often highly complex, and seeks to optimise performance over the whole working volume or a portion thereof, rather than optimising performance of a particular task. In this paper, a method for iteratively teaching poses on a standard industrial robot is presented, and an investigation into the limits on the achievable pose accuracy and the required recalibration period is conducted. Through experimental work on a KUKA KR 240 R2900 ultra robot equipped with a drilling end-effector and measured in 3DoF using a laser tracker, it is demonstrated that the achievable accuracy approaches the stated repeatability of the robot. Finally, investigation results into the accuracy of the robot over short distances to allow small corrections to be applied from these taught poses to compensate for work-piece alignment or thermal effects are presented.

Introduction

Robot calibration is the process of improving the accuracy and repeatability of a robot by identifying and quantifying the sources of inaccuracies, and compensating them to improve the kinematic and dynamic models of the robot. Robot calibration has helped in increasing the usage of robotic arms not only in pick-and-place tasks but also in machining of components, even as far as aerospace components [1]. However, their usage is still limited by their lack of absolute accuracy. Robot calibration can be split between parametric and non-parametric. The parametric calibration considers the kinematic and dynamic modelling of the robot and the parameters those models depend on. The aim of parametric calibration is to identify and estimate the relevant parameters with the purpose of optimizing performance. On the other hand, the non-parametric calibration is concerned with compensating for the errors observed in robot configuration (e.g. errors in Cartesian space) without consideration of the kinematic and dynamic model. This is mostly done by observing the differences between the target and attained pose. In this paper, the results of improving the accuracy of a KUKA KR240 R2900 ultra robot in 3DoF through iterative teaching, i.e. non-parametric calibration, are presented.

Most of the academic research work conducted on robot calibration has concentrated around kinematic calibration. In [2] the authors concentrate on offering a calibration solution by monitoring the coordinate location of a robot manipulator's end effector. In order to achieve the improvement in accuracy, a kinematic calibration approach is implemented such that the errors in end effector location are utilised to optimise the kinematic model of the robot. Two compensation algorithms are used for improving the accuracy once the errors in the kinematic model were identified: the differential error transform and Newton-Raphson compensation method. These approaches only took into consideration geometrical sources of error, as it is to be expected from a kinematic calibration method. The algorithms are further experimentally proven on a six axis PUMA 560 robot, on three data sets. The improvement in Cartesian accuracy noted by the authors was 70% between the calibrated and non-calibrated results. The work done in [2] is a typical example of using a kinematic calibration method.

Laser trackers are often used in literature for identifying the location of a robot and in particular the robot's end effector with respect to its base. In [3] the authors used such a method in order to identify the errors in the end effector positioning of a Motoman SK 120 robot manipulator. Three robot orientations were used in order to demonstrate their method. The authors utilised a laser tracker for the work that has a measurement uncertainty of around 60 microns. Compared to [2], in [3] the authors used the ISO 9283 standards for robot accuracy and robot repeatability to demonstrate their calibration method, as such presents a good reference methodology for any future testing and helps with the comparison of results.

In 2004, Elatta et al presented an overview in robot calibration [4]. The authors classify the calibration methods into model based parametric calibration and model based non-kinematic calibration. The parametric calibration is also known as kinematic and non-kinematic calibration for which three steps are identified: modelling, measurement, and identification and compensation. The non-kinematic calibration is associated with calibration where the sources of error are mechanical sources. The authors of [4] further claim that the kinematic modelling is assuming the robot manipulators links are rigid bodies while the non-kinematic modelling is assuming links to

be non-rigid bodies. The paper mainly discussed the theory behind robot calibration (i.e. methods of robot calibration) without necessarily giving examples of applications.

In [5] assessment methodologies for positioning performance of an ABB IRB1600 robot manipulator are discussed. The paper is concerned with providing a comparison of capabilities between three measurement systems: a laser tracker system, a laser interferometer system and a telescopic ballbar system. The methodology follows the ISO 9283 standards. According to the ISO 9283 standards, the robot being tested should be loaded at its maximum payload. Nevertheless, the tests were conducted with only 1.9 kg of payload (the max payload for the IRB1600 robot is 6 kg) as previous tests conducted (not presented) showed no influence in the robot's repeatability when the payload was increased from 3 kg to 6 kg. The concluding results presented were summarised and the ballbar system was underlined as being more fit for purpose than the other two. Thermal effects were also reported on and it was concluded that the robot needed a long warm up cycle (24hrs in their case) in order for the repeatability measurements to stabilise.

The work conducted in [6] is concerned with improving accuracy of robots for usage in the robotic machining field. The used method is dependent on robot model which makes it difficult to define a homogenous framework for improving accuracy in robotic machining. Compliance and backlash are found to be the dominant sources of error in robotic machining. The authors characterise the sources of error in robotic machining. The robot used for the conducted experiments is a KUKA KR125 that is controlled via a Beckhoff TwinCat controller (CNC controller).

Most recently, in [7], a kinematic calibration methodology for a KUKA KR500 robot was presented. The method is dependent on firstly defining the kinematic model of the used robot (by using the Denavit-Hartenberg (D-H) method). The next step was to define the relationship between the robot coordinate system and the measurement device (API Radian laser tracker) coordinate system. This was done by using the motion around only two axis, A1 and A2. The novelty in the method was that a two-step error model was used. This was utilised to calibrate the D-H kinematic parameters, angle and distance. The authors of [7] compared their newly introduced calibration method to the full parameter calibration method. In the full parameter method, the angles and the distance errors are considered simultaneously.

As stated before, non-kinematic robot calibration takes into account error sources such as stiffness, joint-compliance and friction. Work conducted in non-kinematic robot calibration is considerably less in volume than the work conducted in kinematic robot calibration. This is due in part to the fact that non-kinematic error sources are more difficult to model.

In [8], the authors present a hybrid robot calibration method such that it takes into account kinematic modelling and kinematic sources of error (i.e. geometry based) but also joint and link compliance errors (i.e. non geometry based). For the study, a Staubli TX60L robot manipulator was considered. The non-kinematic errors were modelled through a robot compliance method, specifically by looking into the relationship between torque and tension. In [8] the authors present results supporting that joint compliance errors are more significant in terms of their effect of positional accuracy than link compliance errors. This further informed the use of superposition theory as a robot compliance error analysis method. As such, each joint was modelled as a linear torsional spring with one stiffness coefficient to be identified. Furthermore, it is stated in [8] that the error model for the robot is nonlinear.

Planar constraints are used in [9] in order to develop a non-kinematic robot calibration method. The authors identify the stiffness of the joints of the robot and the kinematic parameters in a simulated environment. The robot considered in the study was a FANUC LR Mate 200iC. The data used for training of their proposed model of calibration was obtained using a precision touch probe. Linear Taylor approximation is used for identifying the stiffness of the robot joints and the kinematic parameters.

The papers considered so far have the kinematic and non-kinematic calibration approach in common. The issue with the kinematic and non-kinematic calibration approaches is that it is not user friendly and it requires deep technical knowledge of robot modelling for implementation. This makes both of them an unattractive calibration method for industrial applications. Furthermore, it may not be necessary to optimise performance over the whole working volume. This is why, in this work, a non-parametric approach was considered for improving robot accuracy through iterative teaching.

In the first instance, the robot was iteratively taught poses to correct for errors attributed to geometric effects. This was followed by investigation of the robot's accuracy over small scales during which it was noted that these errors do not accumulate over a distance of approximately 10 mm and therefore small corrections for errors such as workpiece alignment might be applied without compromising the accuracy of the taught pose.

The next section of the present paper will cover the description of the equipment used and the setup decided upon as well as the method of data gathering. Following this section, the results of the work conducted will be presented. The paper will conclude with a discussion section.

Methodology

Equipment and Setup

The experimental setup is based on a robotic drilling cell with a flexible fixture created for an aerospace project. The cell can be seen in Figure 1 below.

Figure 1. Flexible robotic drilling cell illustrating working volume utilised in the experiment.

The cell consists of a KUKA KR240 R2900 ultra robot with a drilling end-effector fitted with a Leica T-Mac probe to facilitate measurement of the robot pose. The drilling end-effector weighs approximately 120kg, and was kept on during the experiments as realistic payload. The cell also contains a flexible fixturing frame with suction cups, a robot tool changer station (not visible in the picture) and rotary table.

The KUKA KR240 R2900 ultra robot has a maximum payload of 240 kg, a rated repeatability of ±60 µm and a maximum reach of 2896 mm [10]. However, the working range of the robot during the conducted experiments was determined by the cell layout. Before each experiment, the robot was warmed up for a total of 40 minutes by moving it around in each axis within its working volume.

A Leica AT960 absolute laser tracker was used to measure the position of the T-Mac probe and robot TCP (Tool Centre Point), defined as the furthest point along the spindle axis with respect to the robot tool flange. The Leica AT960 and T-Mac probe has a maximum permissible error of ±15 µm + 6 µm/m and was used in conjunction with Spatial Analyser (SA) software to measure the pose of the robot in three degrees of freedom within a USMN (Unified Spatial Metrology Network) coordinate system established by spherically mounted retroreflectors affixed within the cell.

During the experiment, the robot was programmed to sequentially visit 81 different poses within a 600 mm x 1600 mm x 400 mm region directly above the fixture and evenly distributed over 3 x 9 x 3 grid (x, y, z). In each of the poses the end-effector was kept in a downward orientation to mimic a realistic positioning for a drilling application. The robot revisited each of these poses 30 times in order to allow a reliable calculation of the mean attained pose. The error between the mean attained pose and the command pose was then used to correct the future command pose in three subsequent iterations of calibration.

To investigate the pose accuracy over small distances, a Renishaw XL-80 laser was used (see Figure 2). The Renishaw XL-80 device is a laser interferometer typically used to calibrate linear axes within computer numerically controlled machines and has a rated accuracy of ±5 µm per metre. As the device only measures the displacement along a single axis between the laser head and retroreflector, the experiments were separated into three individual sets for the x, y and z axis. The robot was programmed to move 200 mm in 1 mm increments along the x, y or z axis from poses within the working volume where the robot did not have to change configuration or pass through singularity, before returning along the same path. This routine was repeated 30 times to allow a reliable calculation of the mean attained pose at each increment. The increased resolution of the Renishaw device over the laser scanner afforded measurement of errors arising from non-geometrical effects such as backlash in the joints.

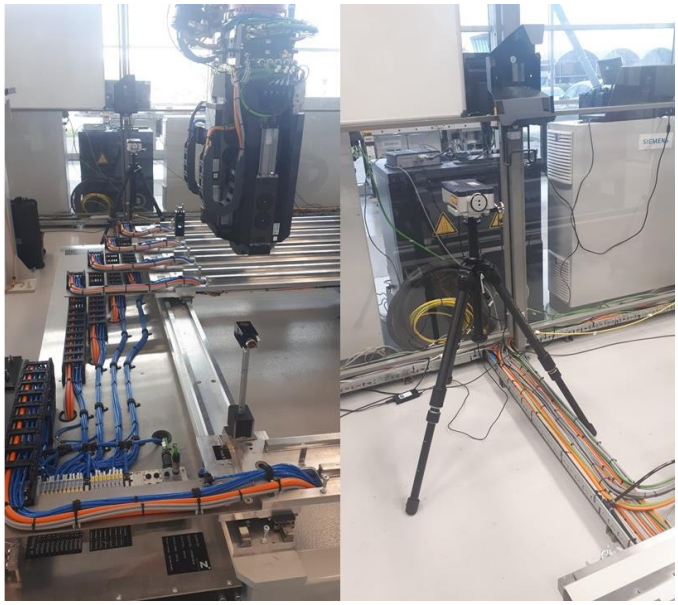

Figure 2. Renishaw XL-80 laser placed within robot cell (left) Renishaw XL-80 laser layout with two optics (right).

Results

Large volume accuracy results

In Figure 3, Figure 4 and Figure 5, the error in each axis is presented by calibration step. The first step is the initial error observed with no calibration applied; Step 2, 3 and 4 represent each of the three calibration steps, and Step 5 represents the error one week after calibration. It can be observed in all plots that the calibration is still valid after a period of one week.

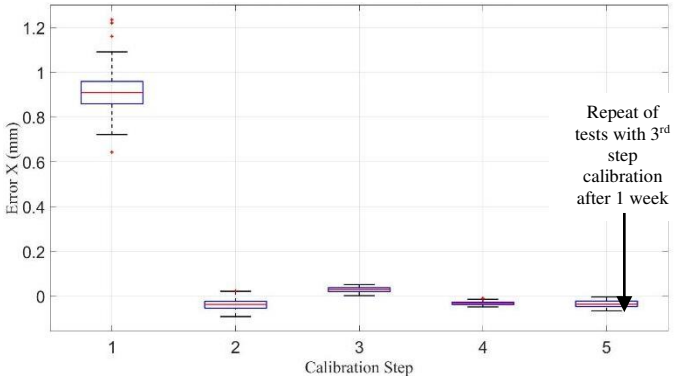

Figure 3. Error by calibration step for X axis.

Figure 3 shows the error by calibration step for the x axis. The red line represents the median of the data points (50% quantile), the top of the rectangle represents the 75% quantile and the bottom of the rectangle represents 25% quantile. The top and bottom whiskers are the maximum and minimum values of the data points. The red points represent outliers.

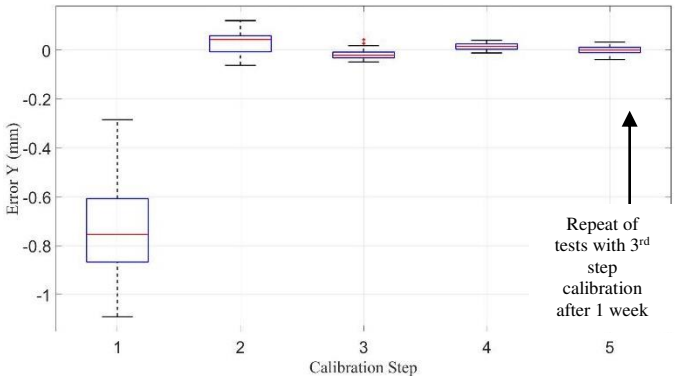

Figure 4. Error by calibration step for Y axis.

Figure 4 shows the error by calibration step for the y axis. As with Figure 3, the red line represents the median of the data points, while the top and bottom of the rectangle represents the 75th percentile and the 25th percentile respectively. The top and bottom whiskers are the maximum and minimum values of the error.

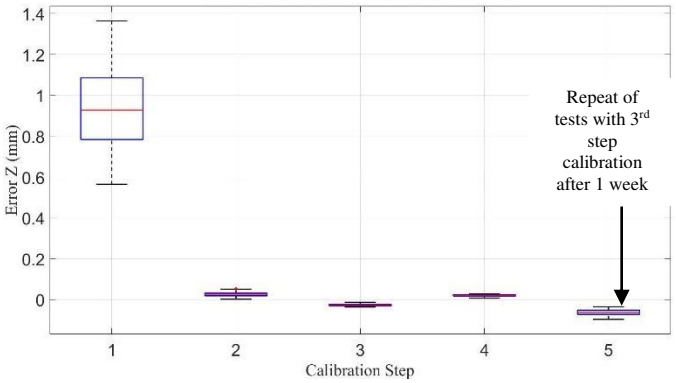

Figure 5. Error by calibration step for Z axis.

Figure 5 shows the error by calibration step for the z axis. The graphical representation is the same as with Figure 3 and Figure 4 such that the red line is the 50% quantile and the bottom and top of the rectangular box is the 25% and 75% quantile. The ends of the whiskers represent the minimum and maximum values of the data points considered.

For all three axis, it can be observed that the spread of the data in the non-calibrated case is considerably bigger than after the robot was calibrated. The first, second and third calibration steps show that the error is getting closer to zero.

To aid visualisation, the deviations from the target pose in the non-calibrated and calibrated states are shown in Figure 6. The overall positional accuracy $A_p$was calculated according to ISO 9283:1998 by using equation (1) below:

$$A_p = \sqrt{(\underline{x} - x_c)^2 + (\underline{y} - y_c)^2 + (\underline{z} - z_c)^2} \quad (1)$$

where, $\underline{x}$, $\underline{y}$, $\underline{z}$ are the coordinates of barycentre of the cluster of poses attained after repeating the same command pose x_c, y_c, z_c 30 times.

Figure 6 (top) shows the colour map for absolute error (from equation (1)) for the non-calibrated robot created by linearly interpolating between the measurement poses. The colour map is plotted for the three attempted x target positions, 800 mm, 1100 mm and 1400 mm respectively. For this case, the maximum error obtained was over 1.8 mm and it corresponded to the target position [x y z] = [1400 400 250]. Figure 6 (bottom) represents the colour map for the absolute error after the third calibration step was conducted. The maximum error obtained after the third step of calibration was approximately 0.058 mm and corresponded to the target position [x y z] = [1400 600 450]. In both panels it can be seen that the pose accuracy varies across the working volume which may be attributed to discrepancies between the actual kinematics of the robot and the idealised model used within the controller which manifests as a pose dependent error. Nevertheless, the non-parametric approach has reduced the maximum error to 0.058 mm.

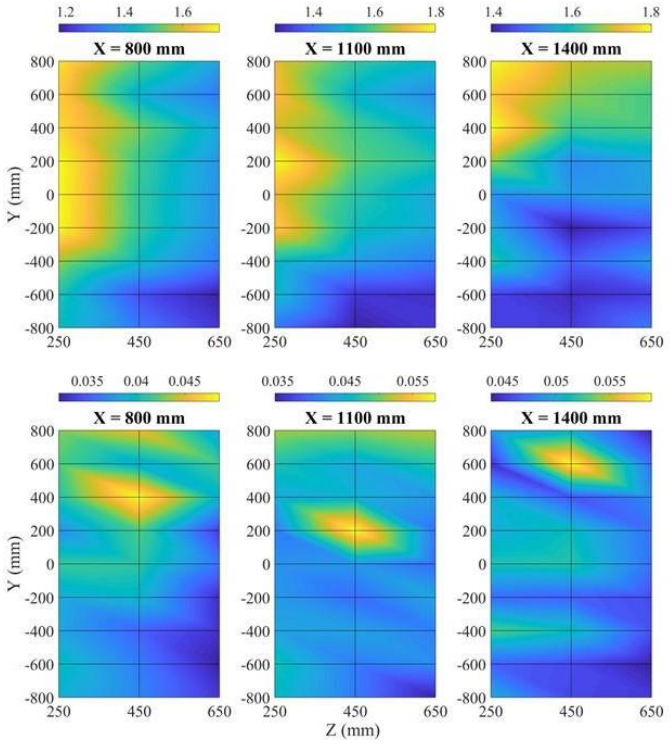

Figure 6. Colour map of absolute error for non-calibrated robot (top) and third step of calibration (bottom).

Figure 7 represents the positional accuracy by calibration step. Once again, the pose accuracy improves dramatically from the first calibration step. Thereafter the spread of the data improves over each subsequent calibration step. From the results of Step 5 one can conclude that even after a period of one week after which time the maximum error observed was 0.1 mm, the calibration is still valid. As such it can be concluded that depending upon the process requirements, the necessary recalibration period may exceed weeks.

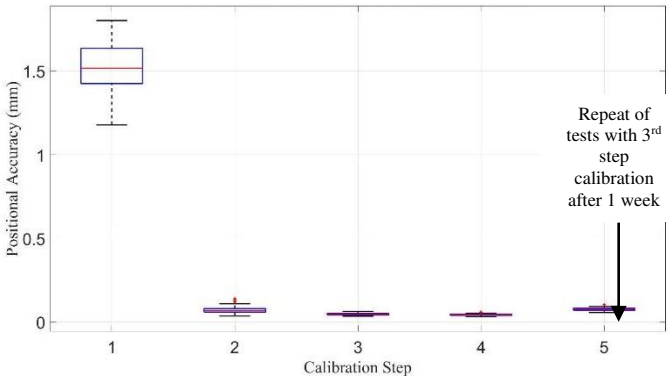

Figure 7. Positional accuracy by calibration step.

Figure 8 presents three times the standard deviation in pose accuracy for at each calibration step, such that 99.7% of the data points were taken into consideration.

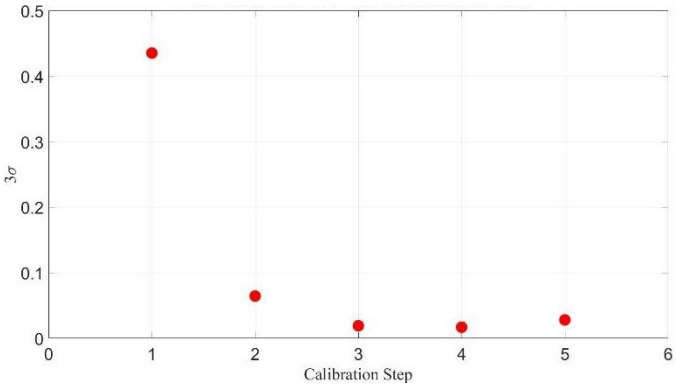

Figure 8. Standard deviations vs Calibration Step.

From Figure 8 the confidence in attaining the target pose improves with each calibration step. This gradual improvement can be related back to the variation in pose accuracy across the working volume in Figure 6: whilst over the working volume the robot may exhibit poor pose accuracy due to discrepancies between the actual kinematics of the robot and the model used within controller, at each calibration step a progressively smaller correction is applied, and over such distances this effect is diminished.

Small volume accuracy results

To further investigate the length scales over which these errors manifest, the pose accuracy over small distances was measured. Figures 9 to 11 show the average mean results for forward and backward runs for each axis. Whilst no pattern can be observed in the x axis mean errors over the 200 mm, for the y and z axes the mean error is continuously increasing over the considered 200 mm. As such it should be concluded that the pose accuracy deteriorates as the robot travels away from a taught position. Again this can be attributed to an accumulation of errors due to discrepancies between the kinematics of the robot and the idealised model used within the controller. Naturally, these errors will be highly dependent upon the joints involved in the movement and thus will vary throughout the working volume. However, this result illustrates that a small offset could be applied to a command pose without compromising the accuracy provided care is taken to avoid reversing direction, which from

Figure 9 to 11 introduces errors that might be attributed to backlash within the robot actuators.

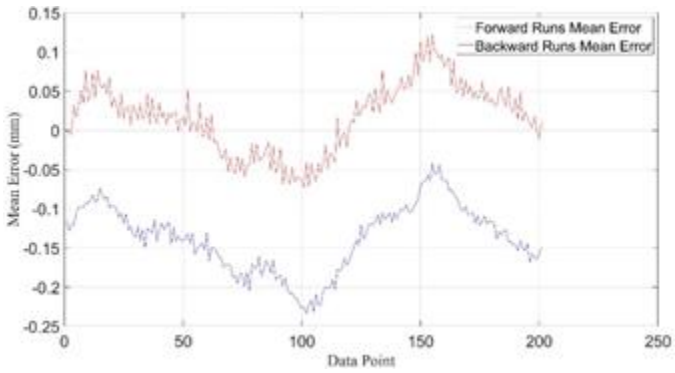

Figure 9. Average error X axis for forward and backward runs.

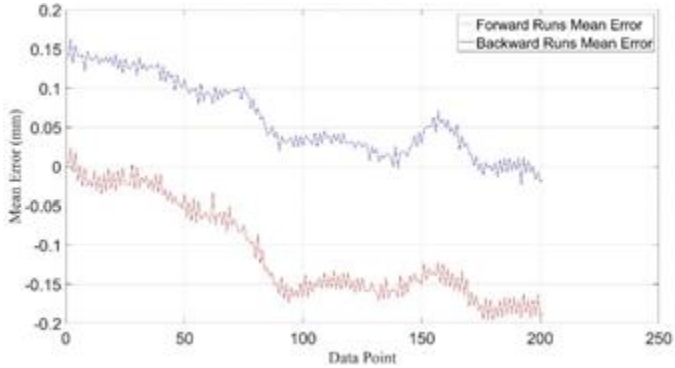

Figure 10. Average error Y axis for forward and backward runs.

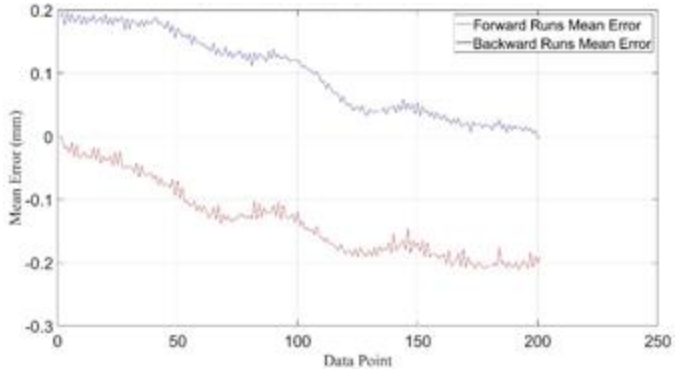

Figure 11. Average error Z axis for forward and backward runs.

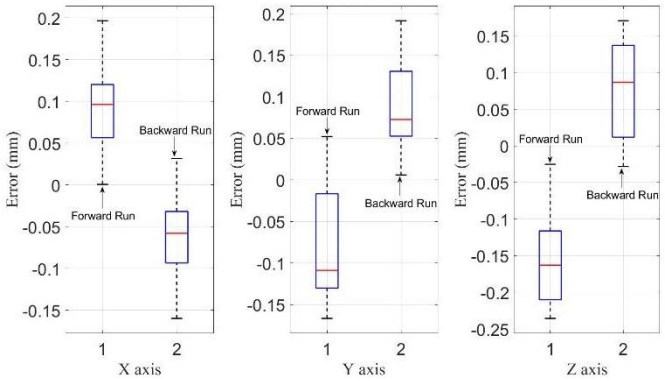

Figure 12. Error per each axis for forward and backward runs.

Figure 12 summarises the pose error per forward and backward run, for each axis. The red line in Figure 12 represents the median of the data points, while the top and bottom of the rectangle represent the 25% and 75% quantile respectively. The top and bottom whiskers are the maximum and minimum of the considered data points. Due to the fact that these tests were run for each individual axis, the presented results in Figure 12 are also given for each individual axis. The difference between the medians of the forward and backward runs in Figure 12 also give an indication of the average reversing error observed.

In Figure 13 the average reversing error along each axis is summarised. For the x axis, an average error of 0.154 mm was observed. For the y axis, the average error was 0.174 mm, while the highest average error was observed on the z axis and it was 0.232 mm.

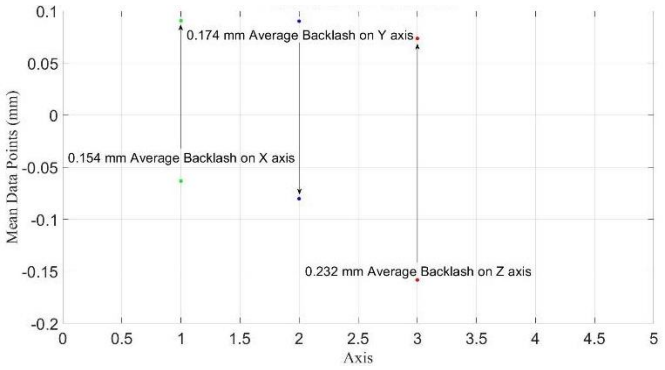

Figure 13. Average backlash observed on each axis.

Conclusions and Discussion

The purpose of the work presented in this paper was to provide an approach for improving robotic accuracy through iterative teaching. The literature shows that the issue of robot calibration is extensively attempted through the use of kinematic and non-kinematic models. However, kinematic and non-kinematic robot calibration approaches require a deep technical knowledge and modelling of the kinematics and dynamics models of the robot. This in turn makes these approaches cumbersome and as such are less likely to be accepted in industry. In this work non-parametric improvements of robot accuracy were discussed and results were presented for the applied methodologies in a large and small working volumes of the KUKA KR240 R2900 ultra robot.

The results presented in the previous section show that after three steps of calibration the robot's positional accuracy improved beyond its stated repeatability, with a maximum error of approximately 0.058 mm. Furthermore, after a time period of one week, the calibration was still valid and the robot's positional accuracy was still close to its stated repeatability, with a maximum error of 0.1 mm. This therefore brings the performance of this standard robot within the typical tolerances of 0.25 mm required of aerospace [11].

Investigation of the robot's performance over small scales revealed that the robot's positional error in each of the three axis does not fluctuate much within 10 mm distance or so of the start point, previously taught using our iterative process. This suggests that small corrections for factors such as workpiece alignment could be applied to the previously taught positions without compromising the pose accuracy provided that care is taken to avoid introducing reversing errors.

Future work will focus on validating the proposed methodology in a representative drilling application and investigation of the resolution limit of the robot in compensating for thermal or other environmental effects.

References

1. Moller, C., Schmidt, H. C., Koch, P., et al, "Machining of large scaled CFRP-Parts with mobile CNC-based robotic system in aerospace industry," *Procedia Manufacturing,*14:17-29,2017, doi: 10.1016/j.promfg.2017.11.003.
2. Veitschegger, W. K., and Wu, C. H., "Robot Calibration and Compensation," *IEEE Journal of Robotics and Automation*. 4(6):643:656, 1988, doi:10.1109/56.9302.
3. Alici, G., and Shirinzadeh, B., "A systematic technique to estimate positioning errors for robot accuracy improvement using laser interferometry based sensing," *Mechanism and Machine Theory*. 40(8): 879-906, 2005, doi: 10.1016/j.mechmachtheory.2004.12.012.
4. Elatta, A. Y., Gen, L. P., Zhi, F. L., et al, "An Overview of Robot Calibration," *Information Technology Journal.* 3(1):74-78, 2004, doi:10.3923/itj.2004.74.78.
5. Slamani, M., Nubiola, A., and Bonev, I., "Assessment of the positioning performance of an industrial robot," *Industrial Robot: An International Journal.* 39(1):57-68, 2012, doi: 10.1108/01439911211192501.
6. Schneider, U., Drust, M., Ansaloni, M., et al, "Improving robotic machining accuracy through experimental error investigation and modular compensation," *The International Journal of Advanced Manufacturing Technology*. 85(1-4):3-15, 2016, doi: 10.1007/s00170-014-6021-2
7. Zhang, J., Wang, X., Wen, K., et al, "A simple and rapid calibration methodology for industrial robot based on geometric constraint and two-step error," *Industrial Robot: An International Journal*. 45(6):721-751, 2018, doi: 10.1108/IR-05-2018-0102
8. Xiaoyan, C., Qiuju, Z., and Yilin, S., "Non-kinematic calibration of industrial robots using a rigid-flexible coupling error model and a full pose measurement method," *Robotics and Computer-Integrated Manufacturing*. 57:46-58, 2019, doi: 10.1016/j.rcim.2018.07.002.
9. Joubair, A., and Bonev, I. A., "Non-kinematic calibration of a six-axis serial robot using planar constraints," *Precision*

Engineering, 40:325-333, 2015, doi: 10.1016/j.precisioneng.2014.12.002
10. KUKA Robotics, "Manual KUKA Series 2000," 2019.

11. DeVlieg, R. and Szallay, T., "Improved Accuracy of Unguided Articulated Robots," *SAE Int. J. Aerosp.* 2(1):40-45, 2010, doi: 10.4271/2009-01-3108.

Contact Information

Daniela Sawyer
The University of Sheffield-AMRC
Factory 2050
Integrated Manufacturing Group
Europa Avenue
Sheffield, S9 1ZA
United Kingdom
www.amrc.co.uk
d.sawyer@amrc.co.uk

Acknowledgments

The present work was possible through HVM CATAPULT funding. The authors are grateful for all the support received during the conducted work. Special thanks to Sam Cowley for the help provided during the experiment period.

Definitions/Abbreviations

SA	Spatial Analyser
USMN	Unified Spatial Metrology Network
DoF	Degree of Freedom
CNC	Computer Numerical Control
D-H	Denavit-Hartenberg
AMRC	Advanced Manufacturing Research Centre